



**HAL**  
open science

## Genetic variant of SRF-rearranged myofibroma with a misleading nuclear expression of STAT6 and STAT6 involvement as 3' fusion partner

Nihous Hugo, Nicolas Macagno, Baud-Massière Jessica, Haffner Aurélie, Jouve Jean-Luc, Gentet Jean-Claude, Touzery Camille, François Le Loarer, Corinne Bouvier

### ► To cite this version:

Nihous Hugo, Nicolas Macagno, Baud-Massière Jessica, Haffner Aurélie, Jouve Jean-Luc, et al.. Genetic variant of SRF-rearranged myofibroma with a misleading nuclear expression of STAT6 and STAT6 involvement as 3' fusion partner. *Virchows Archiv*, 2020, 10.1007/s00428-020-02859-9. hal-03151963

**HAL Id: hal-03151963**

**<https://amu.hal.science/hal-03151963>**

Submitted on 2 Mar 2021

**HAL** is a multi-disciplinary open access archive for the deposit and dissemination of scientific research documents, whether they are published or not. The documents may come from teaching and research institutions in France or abroad, or from public or private research centers.

L'archive ouverte pluridisciplinaire **HAL**, est destinée au dépôt et à la diffusion de documents scientifiques de niveau recherche, publiés ou non, émanant des établissements d'enseignement et de recherche français ou étrangers, des laboratoires publics ou privés.

# Genetic variant of SRF-rearranged myofibroma with a misleading nuclear expression of STAT6 and STAT6 involvement as 3' fusion partner

Hugo Nihous<sup>1</sup> · Nicolas Macagno<sup>1</sup> · Jessica Baud-Massière<sup>2</sup> · Aurélie Haffner<sup>1</sup> · Jean-Luc Jouve<sup>3</sup> · Jean-Claude Gentet<sup>4</sup> · Camille Touzery<sup>5</sup> · François Le Loarer<sup>2</sup> · Corinne Bouvier<sup>1,6</sup>

## Abstract

Pediatric neoplasms with a myofibroblastic differentiation are frequent in children, in particular myofibroma. Recently, a novel deep soft tissue myofibroblastic neoplasm has been described with high cellularity, a smooth muscle phenotype and *SRF-RELA* fusion. We report the case of a 15-year-old boy who presented with a tumor of the deep soft tissue of the arm, with overlapping histological features with the recently described *SRF-RELA* group of myofibromas but differing by the presence of calcifications, a novel *SRF-STAT6* fusion transcript and nuclear expression of STAT6. No local recurrence nor distant metastasis was detected at the current follow-up of 29 months. The clinical relevance of this novel fusion requires further investigations.

**Keywords** SRF · RELA · STAT6 · Pediatric · Leiomyoma · Smooth muscle neoplasm · Myofibroma · Myopericytoma · Myofibroblastic proliferation

## Introduction

In children, the most frequent sarcoma with muscle differentiation is rhabdomyosarcoma. Sarcomas harboring a smooth muscle phenotype, such as leiomyosarcoma, are conversely much more uncommon in children, accounting for 2–4% of soft tissue sarcomas [1]. Their benign counterpart, namely, pediatric leiomyoma, is even more exceptional. Most leiomyomas arise in adult women, in a gynecological context. Leiomyoma of the deep soft tissue (LDST) is a rare neoplasm, accounting for 4% of all benign soft tissue tumors [2].

In contrast to smooth muscle tumors, neoplasms with a myofibroblastic differentiation are much more common in children, in particular myofibroma, which usually harbor *PDGFRB* mutations [3]. A subset of cellular myofibromas of the deep soft tissues have been recently characterized by fusions of *SRF-RELA* or *SRF-ICAIL*, with potential prognostic implications [4, 5]. In contrast to conventional myofibromas, these SRF-rearranged neoplasms display a high cellularity and myoid phenotype.

In this report, we present the case of a 15-year-old boy that developed a deep soft tissue tumor of the arm, expressing a full smooth muscle phenotype and harboring a *SRF-STAT6* fusion transcript, a fusion which had not been reported in this spectrum of neoplasm yet. This case is of potential interest as it also displayed nuclear expression of *STAT6*, a potential diagnostic pitfall with solitary fibrous tumors.

---

✉ Corinne Bouvier  
corinne.Bouvier2@ap-hm.fr

<sup>1</sup> Department of Pathology, INSERM, MMG, APHM, CHU Timone, Aix Marseille University, Marseille, France

<sup>2</sup> Department of Pathology, Institut Bergonié, Bordeaux, France

<sup>3</sup> Department of Pediatric orthopedic, APHM, La Timone Children's Hospital, Marseille, France

<sup>4</sup> Department of Pediatric Hematology and Oncology, APHM, La Timone Children's Hospital, Marseille, France

<sup>5</sup> Department of Radiology, APHM, Hopital Nord, Marseille, France

<sup>6</sup> Service d'Anatomie & Cytologie Pathologiques, Neuropathologie, CHU Timone, Rue Saint-Pierre, 13005 Marseille, France

## Materials and methods

### Immunohistochemistry

Immunohistochemical studies were performed on 4 µm sections cut from the paraffin block using a fully automated system (Benchmark XT System; Ventana Medical Systems Inc.,

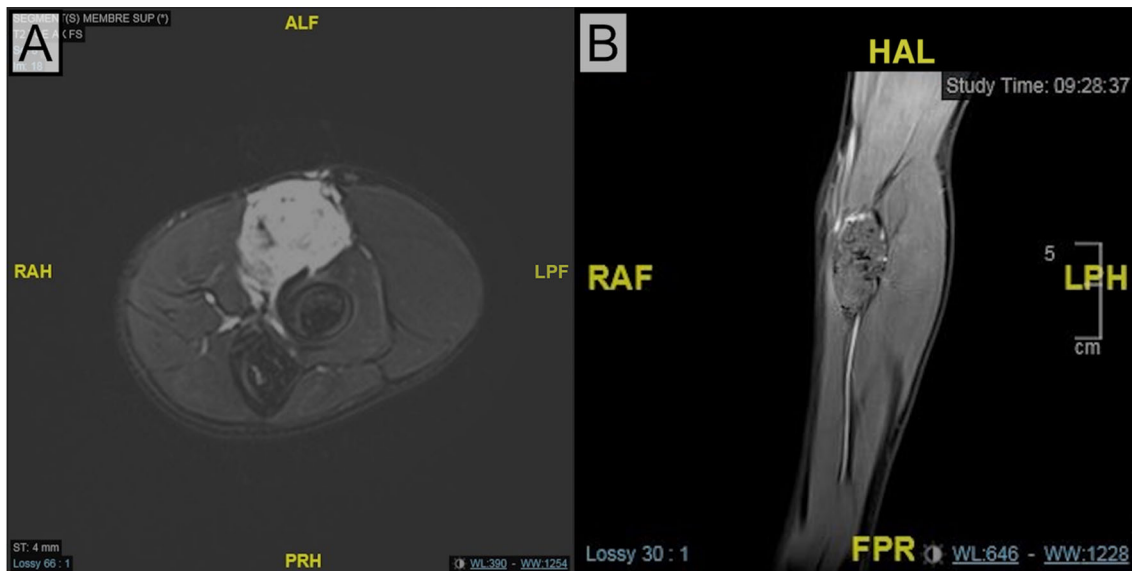


**Fig. 1** MRI of the forearm: **a** (Axial T2 FS (fat-suppressed)). Hyperintense signal of a well-limited oval formation, with stellar and punctiform central calcifications. This formation is located on the external side of the distal part of humeral artery, and in front of the insertion of brachial biceps. This lesion extends over  $33 \times 24$  mm on the axial axis.

There is also an edematous infiltration around the periphery of the lesion. **b** (Coronal-enhanced T1 FS). Heterogenous enhancement of the formation, with a higher enhancement around the periphery of the lesion. This lesion extends over  $54 \times 28$  mm on the coronal axis

Tucson, AZ) and the following primary antibodies: smooth muscle actin alpha (clone 1A4, prediluted; Microm), desmin (clone DE-R-11, prediluted; Roche), h-caldesmon (clone h-CD, 1: 2; Dako), calponin (clone h-cp,1: 20000; Sigma), myogenin (clone F5D, 1: 2; Dako), MyoD1(clone EP212, prediluted; Cell Marque), cluster of differentiation 34 (CD34) (clone QBend10, prediluted; Roche), epithelial membrane antigen (EMA) (clone E29, 1: 500; Dako), PS100 (polyclonal, 1: 400; DBS), Fumarate Hydratase (clone J-13, 1: 100; Santa Cruz Biotechnology), Ki67 (clone MIB-1, 1: 100; Dako), and STAT6 (clone YE361, 1: 250; Abcam Cambridge UK).

### Total RNA extraction

Total RNA was extracted from formalin-fixed paraffin-embedded (FFPE) tissues using TRIzol reagent (Invitrogen). RNA quality was assessed by Eukaryote Total RNA Nano Assay (Agilent, cat. No. 5067-1511), and DV200 was determined. RNAs were stored at  $-80$  °C.

### RNA sequencing

Libraries were prepared with 100 ng of total RNA using TruSeq RNA Access Library Prep Kit (Illumina, San Diego, USA). Libraries were pooled by group of 12 samples. Paired-end sequencing was performed using the NextSeq 500/550 High Output V2 kit on Illumina NextSeq 500 platform (Illumina, San Diego, CA). The read length was 75 bp.

Sequencing data (average of 65 million reads per sample) were aligned with STAR on GRCh 38 reference genome. The fusion transcripts were called with STAR-Fusion, FusionMap, FusionCatcher, ERICSCRIPT, and TopHat-fusion and validated if present in fusion list of at least two algorithms.

### Case report

A 15-year-old boy presented with a lump of the left forearm. Radiological investigations revealed a partially calcified mass, developed in the deep soft tissue, between the radial biceps and the *pronator teres*. The mass displayed hypersignal on T2 FS (fat-suppressed) and a heterogeneous contrast enhancement on T1 FS (Fig. 1) MRI sequences. The two main radiological hypotheses were synovial sarcoma and extraskeletal osteosarcoma. Fine-needle biopsy revealed a spindle cell neoplasm, with a low mitotic activity and a smooth muscle morphology and phenotype, without overt malignant criteria. Surgical excision of the mass was performed. Gross examination revealed a well limited white and firm tumor measuring  $5 \times 3 \times 2$  cm with calcifications.

Histologically, the neoplasm showed a fascicular proliferation of moderate cellularity, composed of spindle cells with ample eosinophilic cytoplasm (Fig. 2a, b, c). Neoplastic cells displayed oval monotonous nuclei, with a finely granular chromatin and occasional pinpoint nucleoli. No pleomorphism nor high-grade nuclear atypia were observed. In some areas, a biphasic morphological appearance was identified owing to a higher cellularity and more basophilic cells.

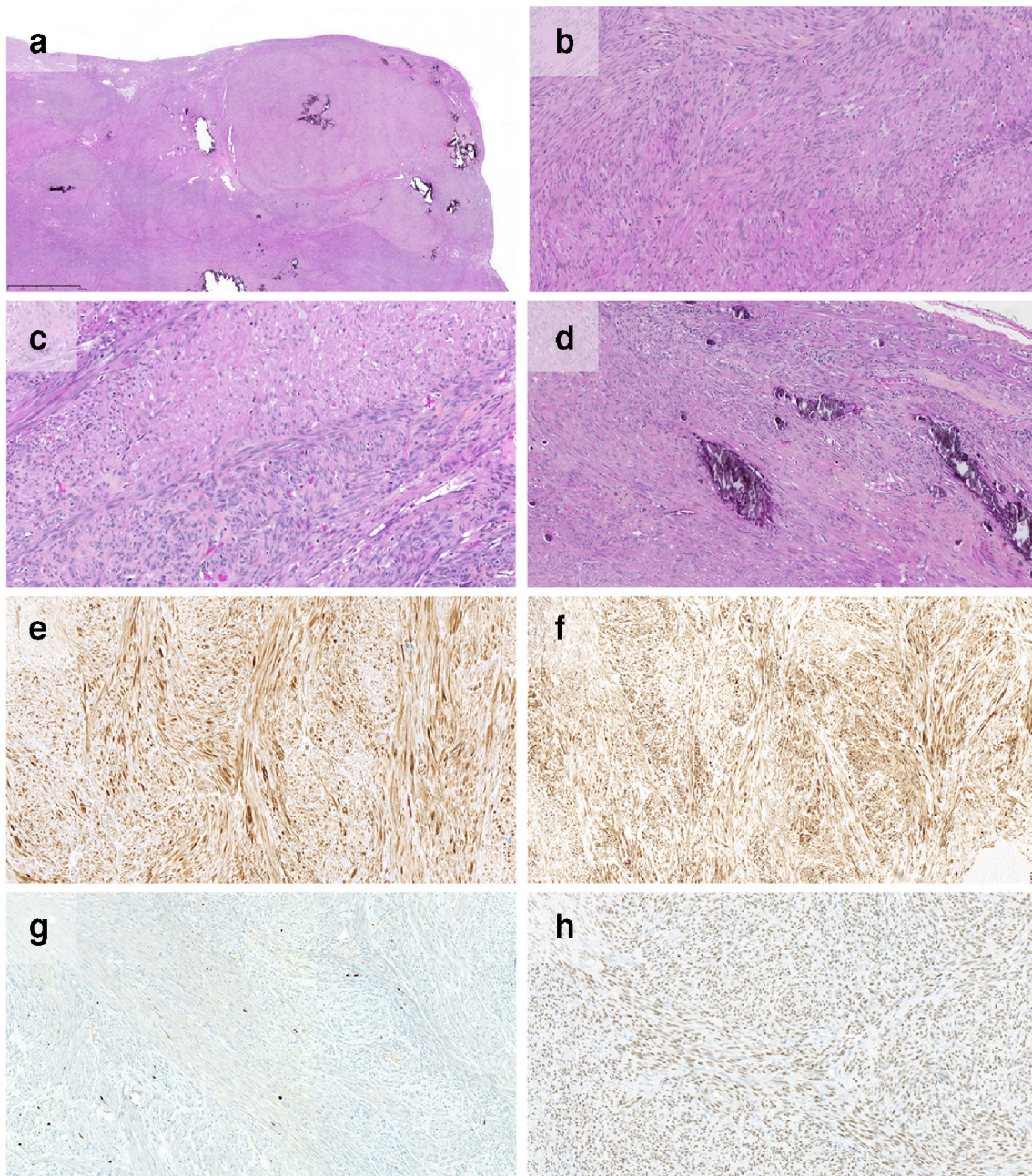


**Fig. 2** Histopathology and immunophenotype: **a** low-power view of the mass, which is well demarcated, without a fibrous capsule, with a multinodular growth of myoid nodules, ectatic vascular channels, and numerous calcifications. Myoid fascicles are intermingled with more cellular area displaying a biphasic architecture. **b** Microscopic detail of a myoid nodule: the proliferation is arranged in fascicles and composed of spindle cells displaying an intermediate myoid-myofibroblastic morphology, associating an eosinophilic myoid, somewhat fibrillar, cytoplasm, and a myofibroblastic central oval and elongated nuclei, with vesicular chromatin, centered by a pinpoint nucleoli. **c** Detail of a hypercellular area: neoplastic cells are more densely packed, smaller, with less

eosinophilic cytoplasm, and darker chromatin details. **d** Calcifications: many small roundish psammomas and calcifications of a larger size are frequently observed, haphazardly distributed within the neoplasm, without being associated with infarction or necrosis. **e** h-caldesmon and **f** desmin are diffusely and intensely expressed, revealing the fascicular architecture of the neoplasm and its smooth muscle phenotype. **g** Ki67 is expressed in 1% of the nuclei; **h** STAT6 is intensely and diffusely expressed in the nuclei, a peculiar finding that is usually observed in the spectrum of solitary fibrous tumors and constitutes a diagnosis pitfall. Of note, nuclei of endothelial cells are negative

Numerous calcifications of variable size were intermingled with tumor cells and were not associated with necrosis (Fig. 2d). Mitotic activity was 1 mitosis per 25 mm<sup>2</sup>. Immunostains revealed diffuse expression of smooth-muscle-actin alpha,

desmin, h-caldesmon, and calponin, without expression of myogenin, MyoD1, CD34, EMA, or PS100 (Fig. 2e–g). The expression of fumarate hydratase was retained, and Ki67 labeling index was 1%.

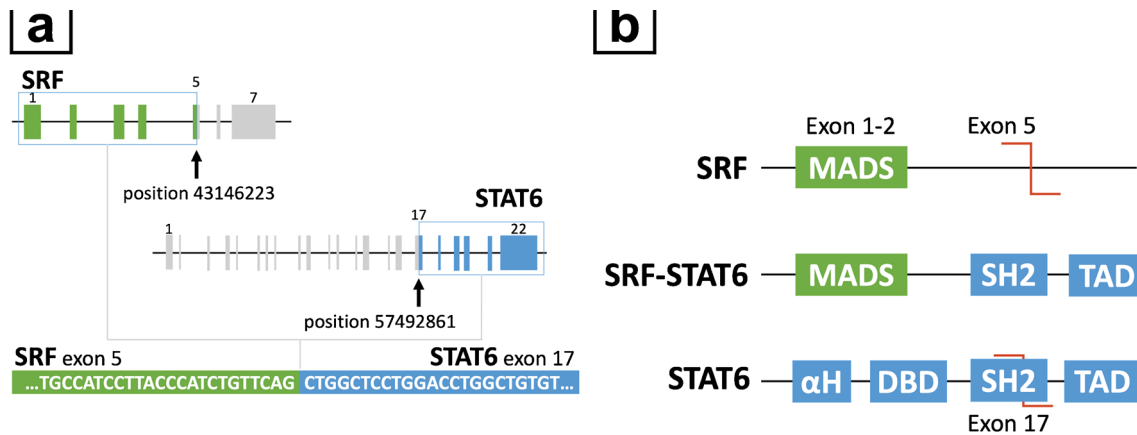


**Fig. 3** Schematic transcript and predicted chimeric protein. **a** *SRF-STAT6* fusion transcript identified by RNA sequencing (RNAseq), representation of the transcript with the identification of the exact breakpoints, occurring at position 4314623 (forward strand) in exon 5 of *SRF* and on position 57492861 (reverse strand) in exon 17 of *STAT6*. **b** Predicted domains of the chimeric protein, the breakpoint within *STAT6* occurs inside the SH2

A provisory diagnosis of “smooth muscle neoplasm of uncertain malignancy” was proposed. Ancillary genetic investigations were performed to assess its aggressiveness. Array-based comparative genomic hybridization revealed no cytogenetic gain nor loss across the tumor genome, raising suspicion for a translocation-related tumor. No genomic breakpoint was stated across genome, especially in *STAT6* nor *SRF* loci. Next-generation sequencing (NGS) revealed no alteration of *TP53* nor *RBI*. Whole genome RNA-sequencing revealed a *SRF-STAT6* fusion transcript (Fig. 3a). Interestingly, the neoplasm displayed a diffuse and intense nuclear expression of *STAT6* by immunohistochemistry (Fig. 2h). No local recurrence nor distant metastasis was detected during a 29-month follow-up.

## Discussion

We report a new fusion involving *SRF* and *STAT6* in a mesenchymal neoplasm with a full smooth muscle phenotype. This case illustrates the recent molecular findings in cellular myoid neoplasms, a subset of which are associated with recurrent fusions involving *SRF* with *RELA*, *C3orf62*, or *ICA1L* [4, 5] (Table 1).

Tumors with rearrangements of *SRF* have been linked to myofibroma and myopericytoma. This group of neoplasm was characterized by a biphasic architecture: spindle cells with abundant eosinophilic cytoplasm arranged in fascicles, alternating with ovoid cells arranged in a syncytial growth or nested architecture, with a rich capillary network. Nuclei were ovoid with fine or vesicular chromatin, without high-grade atypia, and mitotic activity was generally low. In some cases, areas of infarction were present associated with dystrophic

calcifications. These neoplasms expressed a smooth muscle differentiation: all reported cases stained for smooth muscle actin alpha, while desmin and h-caldesmon were more variably expressed [1, 2, 4]. Our case displayed similarities with this group of neoplasm, on both histopathological and immunohistochemical grounds (Table 1). However, our case lacked necrosis associated with dystrophic calcifications. Instead, the calcifications were rather scattered within the proliferation. *SRF-RELA* neoplasms are thought to carry a low risk of recurrence.

A recent report also described another subset of cases with *SRF-ICA1L* fusions, further expanding this group of neoplasms [5]. However, these neoplasms did not express desmin nor h-caldesmon and displayed worrisome histological features, such as an increased mitotic activity and necrosis (Table 1).

Our case harbored a novel translocation, fusing exon 5 of *SRF* with exon 17 of *STAT6*. Serum response factor (SRF) is a member of the MADS box superfamily of transcription factors, which play a role in cell proliferation and migration, muscle development and differentiation, cardiac muscles homeostasis [6], leiomyomatosis, and fumarate hydratase deficiency [7]. Fumarate hydratase-deficient leiomyoma was excluded by immunohistochemistry in our case. *SRF*-fusions have been reported in other mesenchymal neoplasms, such as *SRF-NCOA2* in infantile spindle cell rhabdomyosarcoma [8], *SRF-FOXO1* and *SRF-NCOA1* in a new distinctive subset of well-differentiated rhabdomyosarcoma [9], and *SRF-E2F1* in myoepithelioma [10].

*STAT6* is a cytoplasmic transcription factor, which belongs to the *STAT* family of proteins that regulate gene expression. These key transcription factors are necessary for embryonic development, immune function,

domain. The chimeric protein contains the MAD box domain from *SRF*, a part of the SH2 domain and the C-terminal transactivation domain (TAD) (MADS MAD box domain,  $\alpha$ H alpha-helix domain, DBD DNA binding domain, SH2 Src homology domain 2, TAD transactivation domain)

**Table 1** Summary of the clinicopathologic features of published SRF-rearranged myofibroblastic neoplasms

Study	Fusion transcript	Age/Sex	Location	Size (cm)	Biphasic pattern	Necrosis	Mitotic count (/10 HPF)	Calcifications	Immunohistochemistry				Clinical follow-up
									SMA	DES	H-Cald	CD34	
Present case	SRF-STAT6	15 years/M	Forearm	5	+	-	1	+	+	+	+	-	NED, 29 months
Suurmeijer et al. 2019	SRF-ICAIL	23 years/M	Buttock	11	-	+ <sup>a</sup>	12	+ <sup>c</sup>	+	-	-	-	NED, 5 years
	SRF-ICAIL	49 years/F	Thoracic	8.5	-	-	6	-	+	-	-	-	NED, 2 years
	SRF-ICAIL	55 years/M	Buttock	10	-	+ <sup>a</sup>	13	+ <sup>c</sup>	+	-	-	-	NA
	SRF-ICAIL	35 years/M	Hip	19	-	+ <sup>a</sup>	>20	+ <sup>c</sup>	+	-	-	-	AWD, 7 years
Antonescu et al. 2017	SRF-RELA	8 years/F	Forearm	2.8	+	-	2	-	+	+	+	-	NED, 28 months
	SRF-RELA	3 years/F	Abdominal wall	3	+	-	1	-	+	+	+	-	NED, 42 months
	SRF-RELA	6 years/M	Knee	NA	+	-	1	-	+	+	NA	+	NED, 44 months
	SRF-RELA	28 years/M	Inguinal	7	+	- <sup>b</sup>	1	+	+	+	+	-	NA
	SRF-RELA	40 years/F	Neck	NA	+	- <sup>b</sup>	14	-	+	+	NA	-	NA
	SRF-RELA	63 years/F	Small bowel	4.5	+	-	1	-	-	+	NA	+	NA
	SRF-RELA	13 years/F	Chin	3.5	+	- <sup>b</sup>	8	+	+	+	NA	-	NA
	SRF-C3orf62	0 year/F	Chest wall	1.9	+	-	3	-	+	+	NA	+	NED, 24 months
	SRF	18 years/M	Upper arm	4.5	+	-	10	-	+	+	NA	NA	NED, 42 months
	SRF	0 years/F	Foot	5	+	- <sup>b</sup>	2	+	+	+	NA	NA	NA

HPF high power field, SMA smooth muscle actin alpha, DES desmin, H-CALD H-caldesmon, NA not available, γ year, mo month, F female, M male, NED no evidence of disease, AWD alive with disease

<sup>a</sup> Coagulative tumor necrosis

<sup>b</sup> Areas of infarction

<sup>c</sup> Calcification in cases associated with necrosis

cell differentiation, growth, and apoptosis. *STAT6* protein is composed of a DNA-binding domain, a SH2 domain, and a C-terminal transcriptional activation domain (TAD) (Fig. 3b). In mesenchymal neoplasms, fusions of *STAT6* typically occur in solitary fibrous tumors, for which *NAB2-STAT6* fusions are highly specific [10, 11]. In solitary fibrous tumors, over 40 types of *NAB2-STAT6* fusion proteins have been reported and all the predicted *NAB2-STAT6* fusion proteins retain the C-terminal portion of *STAT6*, which contains the domain of transactivation. The fusion induces a permanent nuclear translocation of this portion of *STAT6*, which is easily detected by immunohistochemistry and widely used for the pathological diagnosis of solitary fibrous tumors [12–14]. In the present case, a similar *STAT6* nuclear immunostaining was observed, representing a potential diagnostic pitfall. Nevertheless, solitary fibrous tumors display a diffuse expression of CD34 and do not display a biphasic pattern nor a myoid cytology. The nuclear overexpression of *STAT6* has also been reported in dedifferentiated liposarcoma, albeit not associated with translocations but rather with amplifications of 12q13 on which *MDM2* and *STAT6* are mapped [15].

In our case, as exon 5 of *SRF* and exon 17 of *STAT6* were involved, the predicted fusion protein contained the MAD box domain of *SRF* and the whole transcriptional activation domain (TAD) of *STAT6* (Fig. 3b): therefore, the predicted chimeric *SRF-STAT6* fusion protein displayed both a DNA binding capacity from *SRF* and a transcriptional activation potential from *STAT6*.

Interestingly, all *SRF-RELA*, *SRF-ICA1L* fusion neoplasms, and the present *SRF-STAT6* case show a similar *SRF* breakpoint, retaining the MADS box domain. Also, the retained parts of *RELA*, *ICA1L*, or *STAT6* within the fusion proteins always contain their respective domain of transactivation.

As this is the only case so far reported, the relationship of this tumor with respect to the *SRF*-rearranged group of myoid neoplasms requires further investigations, in particular its prognostic relevance.

## Conclusion

Altogether we have described a new variant of *SRF*-rearranged neoplasm sharing histological features with the recently described group of *SRF*-rearranged myofibroblastic neoplasms. The case involved *STAT6* as 3' fusion partner, which resulted in a strong nuclear expression of *STAT6*, a potential diagnosis pitfall with solitary fibrous tumors. The clinical relevance of this novel fusion requires further investigations.

**Acknowledgments** The authors thanked Dr. C. Charon-Barra and Dr. R. Boidot for NGS data.

**Author contributions** CB conceived the study, analyzed and acquired the data, then critically reviewed and revised the manuscript.

HN analyzed the data and wrote the manuscript.

AH summarized bibliography of all published cases.

CT refined radiological description and images.

NM analyzed the data, critically reviewed and revised the manuscript.

JLJ and JCG acquired clinical data and critically reviewed the manuscript.

JBM and FLL acquired and analyzed the data, then critically reviewed and revised the manuscript.

All authors gave final approval for publication.

## Compliance with ethical standards

This manuscript is a report of one case with a review of the literature. Research work with human and animal subjects was not conducted in preparation of this manuscript.

**Conflict of interest** The authors declare that they have no conflict of interest.

## References

1. Hoda SA (2014) Enzinger and Weiss's soft tissue tumors, 6th edition. *Adv Anat Pathol* 21:216
2. Kransdorf MJ (1995) Benign soft-tissue tumors in a large referral population: distribution of specific diagnoses by age, sex, and location. *Am J Roentgenol* 164:395–402
3. Agaimy A, Bieg M, Michal M, Geddert H, Märkl B, Seitz J, Moskalev EA, Schlesner M, Metzler M, Hartmann A, Wiemann S, Michal M, Mentzel T, Haller F (2017) Recurrent somatic PDGFRB mutations in sporadic infantile/solitary adult myofibromas but not in angioleiomyomas and myopericytomas. *Am J Surg Pathol* 41:195–203
4. Antonescu CR, Sung Y-S, Zhang L, Agaram NP, Fletcher CD (2017) Recurrent *SRF-RELA* fusions define a novel subset of cellular variants in the myofibroma/myopericytoma spectrum: a potential diagnostic pitfall with sarcomas with myogenic differentiation. *Am J Surg Pathol* 41:677–684
5. Suurmeijer AJ, Dickson BC, Swanson D et al (2020) Novel *SRF-ICA1L* fusions in cellular myoid neoplasms with potential for malignant behavior. *Am J Surg Pathol* 44(1):55–60
6. Miano JM (2010) Role of serum response factor in the pathogenesis of disease. *Lab Invest* 90:1274–1284
7. Raimundo N, Vanharanta S, Aaltonen LA, Hovatta I, Suomalainen A (2009) Downregulation of *SRF-FOS-JUNB* pathway in fumarate hydratase deficiency and in uterine leiomyomas. *Oncogene* 28:1261–1273
8. Mosquera JM, Sboner A, Zhang L, Kitabayashi N, Chen CL, Sung YS, Wexler LH, LaQuaglia MP, Edelman M, Sreekantaiah C, Rubin MA, Antonescu CR (2013) Recurrent *NCOA2* gene rearrangements in congenital/infantile spindle cell rhabdomyosarcoma. *Genes Chromosomes Cancer* 52:538–550
9. Karanian M, Pissaloux D, Gomez-Brouchet A et al (2020) *SRF-FOXO1* and *SRF-NCOA1* fusion genes delineate a distinctive subset of well-differentiated rhabdomyosarcoma. *Am J Surg Pathol* 44:607–616
10. Urbini M, Astolfi A, Indio V, Tarantino G, Serravalle S, Saponara M, Nannini M, Gronchi A, Fiore M, Maestro R, Brenca M, Dei Tos AP, Dagrada GP, Negri T, Pilotti S, Casali PG, Biasco G, Pession

- A, Stacchiotti S, Pantaleo MA (2017) Identification of SRF-E2F1 fusion transcript in EWSR-negative myoepithelioma of the soft tissue. *Oncotarget* 8:60036–60045
11. Doyle LA, Vivero M, Fletcher CD et al (2014) Nuclear expression of STAT6 distinguishes solitary fibrous tumor from histologic mimics. *Mod Pathol* 27:390–395
  12. Robinson DR, Wu Y-M, Kalyana-Sundaram S, Cao X, Lonigro RJ, Sung YS, Chen CL, Zhang L, Wang R, Su F, Iyer MK, Roychowdhury S, Siddiqui J, Pienta KJ, Kunju LP, Talpaz M, Mosquera JM, Singer S, Schuetze SM, Antonescu CR, Chinnaiyan AM (2013) Identification of recurrent NAB2-STAT6 gene fusions in solitary fibrous tumor by integrative sequencing. *Nat Genet* 45:180–185
  13. Demicco EG, Harms PW, Patel RM, Smith SC, Ingram D, Torres K, Carskadon SL, Camelo-Piragua S, McHugh JB, Siddiqui J, Palanisamy N, Lucas DR, Lazar AJ, Wang WL (2015) Extensive survey of STAT6 expression in a large series of mesenchymal tumors. *Am J Clin Pathol* 143:672–682
  14. Cheah AL, Billings SD, Goldblum JR et al (2014) STAT6 rabbit monoclonal antibody is a robust diagnostic tool for the distinction of solitary fibrous tumour from its mimics. *Pathology (Phila)* 46: 389–395
  15. Doyle LA, Tao D, Mariño-Enríquez A (2014) STAT6 is amplified in a subset of dedifferentiated liposarcoma. *Mod Pathol Off J U S Can Acad Pathol Inc* 27:1231–1237

**Publisher's note** Springer Nature remains neutral with regard to jurisdictional claims in published maps and institutional affiliations.